On the significance of magnetic anomalies from the Baja California Peninsula: its relationship with IOCG deposits and the deep crustal magnetic layer

Juan García-Abdeslem

Centro de Investigación Científica y de Educación Superior de Ensenada (CICESE),
División de Ciencias de la Tierra, Departamento de Geofísica Aplicada,
Carretera Ensenada Tijuana No. 3916, Zona Playitas, Ensenada, Baja California, Mexico.
jgarcia@cicese.mx

ABSTRACT

A regional-residual separation process has been applied to aeromagnetic data observed over southern California and the Baja California Peninsula. The 3D analytic signal amplitude computed from the residual magnetic anomalies is intense and delineates a strip ~60 km wide and ~1200 km long characterized by short-wavelength and high amplitude anomalies, that extends from southern California southward nearly to the tip of the Baja California Peninsula. Known iron-oxide-copper-gold (IOCG) ore deposits are for the most part located in the northern portion of the strip, and its eastern boundary closely follows the magnetite-ilmenite boundary. The amplitude and continuity of regional magnetic anomalies, which suggests an almost continuous belt of magnetized rocks, supports a hypothesis suggesting that the western margin of the Baja California Peninsula evolved as an island arc that was accreted to the western margin of North America in Cretaceous time. Inverse modeling of the long-wavelength regional magnetic anomalies indicates that two nearly continuous belts of magnetized rocks, of mafic to intermediate composition, extend from southern California to the La Paz fault. The boundary between these two belts is located near the Bahía de Sebastián Vizcaíno, in a region where magnetization abruptly decreases.

Key words: magnetic anomalies; IOCG deposits; linear inversion; crustal magnetization; Baja California Peninsula; Mexico.

RESUMEN

Un proceso de separación regional-residual fue aplicado a datos aeromagnéticos observados en el Sur de California y en la Península de Baja California. La amplitud de la señal analítica 3D de las anomalías magnéticas residuales es intensa en una franja de ~60 km de ancho y ~1200 km de longitud, también caracterizada por anomalías magnéticas de gran amplitud y corta longitud de onda, que se extiende desde el sur de California hasta casi la punta sur de la Península de Baja California. La mayoría de los depósitos minerales de óxidos de fierro, cobre y oro (IOCG) se localizan en la porción norte de esa franja, cuya frontera oriental coincide aproximadamente con la frontera magnetita-ilmenita. La amplitud y continuidad de las anomalías magnéticas regionales sugiere un cinturón casi continuo de rocas magnetizadas, que apoya una hipótesis que sugiere que la margen occidental de la Península de Baja California evolucionó como un arco de islas que fue acrecionado a la margen occidental de Norteamérica durante el Cretácico. La modelación inversa de las anomalías magnéticas regionales de gran longitud de onda indica que existen dos cinturones casi continuos de rocas magnetizadas, de composición intermedia a máfica, que se extienden desde el sur de California hasta la falla de la Paz. La frontera entre estos dos cinturones se localiza en la región de Sebastián Vizcaíno, en donde la magnetización de la corteza profunda decrece abruptamente.

Palabras clave: anomalías magnéticas; depósitos IOCG; inversión lineal; magnetización de la corteza profunda; Península de Baja California; México.

INTRODUCTION

Aeromagnetic surveys play an important role in the exploration of natural resources of economic interest as well as in regional geologic mapping. Magnetic anomaly maps delineate the lateral variations of magnetization in the crust, and are often characterized by smooth regional features and isolated variations referred to as magnetic anomalies. The main goal of magnetic prospecting is to infer, either by direct or inverse modeling, the geometry and magnetization intensity of the geological bodies causing the observed magnetic anomalies.

As a result of a continuous effort by the Servicio Geológico Mexicano, a complete aeromagnetic map of México has been achieved, with N-S oriented survey lines, spaced 1 km, flown at a nominal elevation of 300 m above the topography. Using these data an aeromagnetic map of México (Lara-Sánchez, 2000) showed a first-order linear magnetic feature of continental scale extending along the entire length of the Baja California Peninsula. It is characterized by its large amplitude, varying between -1000 to 2400 nT – this in contrast with lower amplitude magnetic anomalies observed to the east of this singular region, where values vary around ± 300 nT.

By the year 2002, the Digital Magnetic Map of North America (DMMNA) was achieved as the outcome of a joint project between the Canadian Geological Survey, the United States Geological Survey and the Servicio Geológico Mexicano (NAMAG, 2002). The digital data provide residual, total-field magnetic anomalies with respect of the International Reference Geomagnetic Field, have a spatial (grid cell size) resolution of 1 km, and were acquired (or leveled) at a nominal elevation of 300 m draped above the topography. The data are available

at the United States Geological Survey web site (<http://crustal.usgs.gov/projects/namadat/>). From those data, Langenheim and Jachens (2003) examined a region comprising the southwestern USA and northwestern México to show again the remarkable magnetic anomaly along the Baja California Peninsula. They applied a transformation (Baranov, 1957) to the magnetic anomaly data to obtain a pseudo-gravity anomaly, deducing that a mafic and fairly coherent crustal structure extends all along the Baja California Peninsula, and suggesting that such a crustal block behaved during Cenozoic time as a relatively rigid body that spaced the Cenozoic extension to the Gulf of California Extensional Province.

More recently (García-Abdeslem and Martínez-Cañedo, 2009) carried out several transformations on data from the DMMNA focused on the Baja California Peninsula, and aimed at finding a relationship between residual total-field magnetic anomalies and the distribution of iron-oxide-copper-gold (IOCG) ore deposits (CRM, 1999a, 1999b). It was found that residual magnetic anomalies, characterized by high amplitudes and short wavelengths, are mostly restricted to a ~60 km wide and ~1200 km long strip, where most known IOCG deposits reside, and that the magnetite-ilmenite boundary proposed by Gastil *et al.* (1990) closely coincides with the eastern boundary of the strip.

Figure 1, a simplified geologic map, shows Mesozoic plutonic rocks cropping out along the Peninsular Ranges batholiths (PRB) of southern California and Baja California, north of the Bahía de Sebastián Vizcaíno, and on the Los Cabos block at the southern tip of the Baja California Peninsula. Mesozoic volcanic rocks crop out only along the western continental margin of the Peninsula, north of Sebastián

Vizcaíno. Cenozoic volcanic rocks crop out on several fields including: Las Pintas-Tinajas (~ 33.5°N), Puertecitos (~ 30°N), Jaraguay (~29°N), and the Comondú arc that extends along the southern portion of the Peninsula (~ 28-23°N).

The magnetite-ilmenite boundary (Figure 1) separates magnetite-bearing granitic rocks in the western portion of the PRB from ilmenite-bearing granitic rocks in the eastern portion of the PRB. Using magnetic susceptibility measurements on the batholiths of southern California and Baja California, Gastil *et al.* (1990) traced this boundary southward to the border between Baja California and Baja California Sur states at latitude 28°N. In the western batholiths, the magnetic susceptibility varies between 1×10^{-3} and 1×10^{-1} (SI). In the eastern batholiths the magnetic susceptibility roughly varies between 1×10^{-4} and 1×10^{-3} (SI). Magnetite (Fe_3O_4) is a ferrimagnetic material that looses its magnetization when temperatures rise above its Curie point (~580 °C). Magnetite is generally considered to be the main carrier of the magnetization in the crustal magnetic layer, and consequently the main source of magnetic anomalies. Ilmenite ($FeTiO_3$) is antiferromagnetic, but behaves paramagnetically at room temperature (Tarling, 1983).

In this work I used data from the DMMNA to obtain regional and residual magnetic anomalies over southern California and the Baja California Peninsula, with the following two objectives: (1) to delineate shallow and strongly magnetized regions by the 3D analytic signal amplitude of the residual magnetic anomalies and show their relationship with IOCG ore deposits; (2) to infer and outline the magnetization intensity of the deep crustal magnetic layer along the Baja California Peninsula by 3D linear inverse modeling of the regional magnetic anomalies.
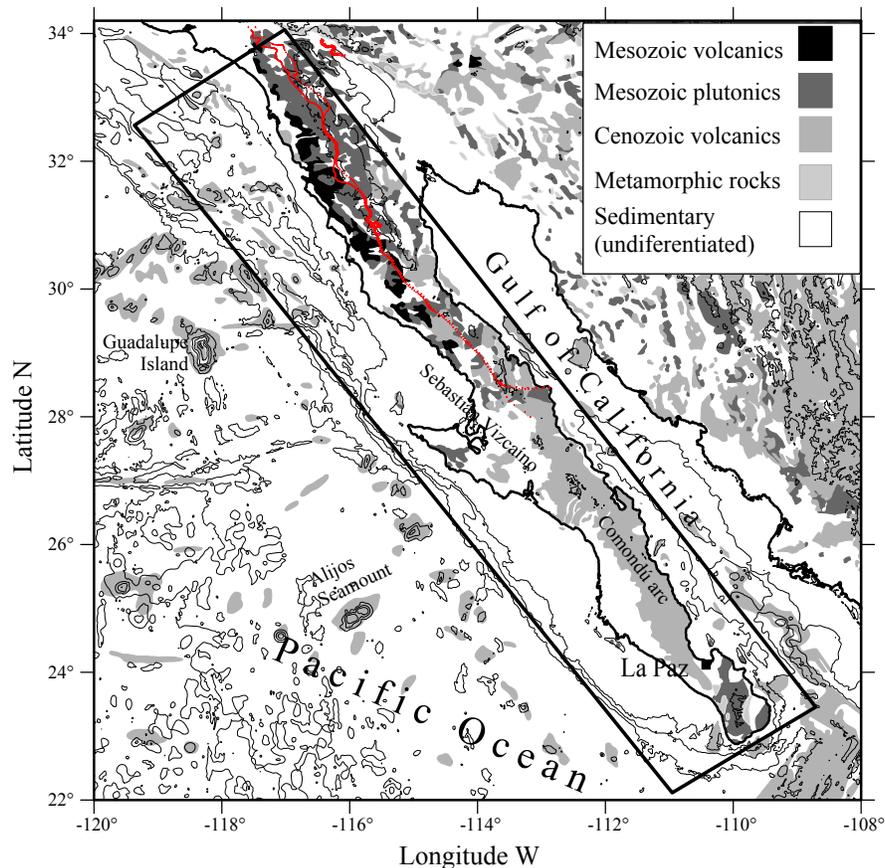

Figure 1. Simplified geologic map of the study area, adapted from USGS (2010). The bathymetry and topography are shown with contour lines every 1000 m. The magnetite-ilmenite boundary was adapted from Gastil *et al.* (1990) and traced by the red solid symbols. The black rectangle indicates the boundaries of Figures 5-7.

REGIONAL-RESIDUAL SEPARATION

The magnetic anomaly data collected in a geophysical survey results from the superposition of the magnetic fields produced by all underground sources. However, depending on the geologic target of the survey it may be convenient to separate the observed magnetic data into a short-wavelength residual field, which is generally attributed to shallow magnetic sources, from the long-wavelength regional magnetic field, attributed to larger-scale and more deeply buried geologic features. The separation of regional and residual magnetic field data is a classical problem in exploration geophysics, and a review of methods to carry on this task is found in Hinze (1990) and Li and Oldenburg (1998).

To separate the total-field magnetic anomaly (Figure 2a) into regional and residual components, the data were represented on a regular grid with nodes separated 1 km and analytically continued 15-km upward to attenuate as much as possible the shallow magnetic response while retaining the long-wavelength regional magnetic anomalies due to the deep crustal magnetic layer (Figure 2b). The residual (Figure 2c) was obtained by subtracting the long-wavelength regional anomalies from the observed aeromagnetic data.

The 3D analytic signal amplitude of residual magnetic anomalies

The 3D analytic signal amplitude (*ASA*) of the residual total field magnetic anomalies, h, (Li , 2006) is given by

$$|ASA(x,y)| = \sqrt{\left(\frac{\partial h}{\partial x}\right)^2 + \left(\frac{\partial h}{\partial y}\right)^2 + \left(\frac{\partial h}{\partial z}\right)^2} \qquad (1)$$

Short-wavelength features characterize the 3D *ASA* that roughly outlines strongly magnetized zones likely related to major concentrations of iron-oxide, and this is shown along with the distribution of IOCG ore deposits in Figure 3.

It is worth noting that most iron-oxide ore deposits have been reported only in the northern portion of the Baja California Peninsula and west of the magnetite-ilmenite boundary, where both the residual magnetic anomalies and their 3D *ASA* have larger amplitudes. In the southern portion of the Baja California Peninsula residual magnetic anomalies and their 3D *ASA* are less intense and mainly follow the Comondú arc (Figure 1). The gold deposits are unevenly distributed, but most copper deposits reside in the region where both the residual magnetic anomalies and the 3D *ASA* have larger amplitude. The distribution of IOCG ore deposits along the western portion of the Baja California Peninsula is similar to other plutonic belts of the Pacific rim, where metallic ore deposits such as chalcopyrite, bornite, sphalerite, galena, and argentite, among others, occur in the form of sulphides, derived from oxidized granitoids of the magnetite series, and gold is found surrounding oxidized plutons (Ishihara, 1977, 2003).
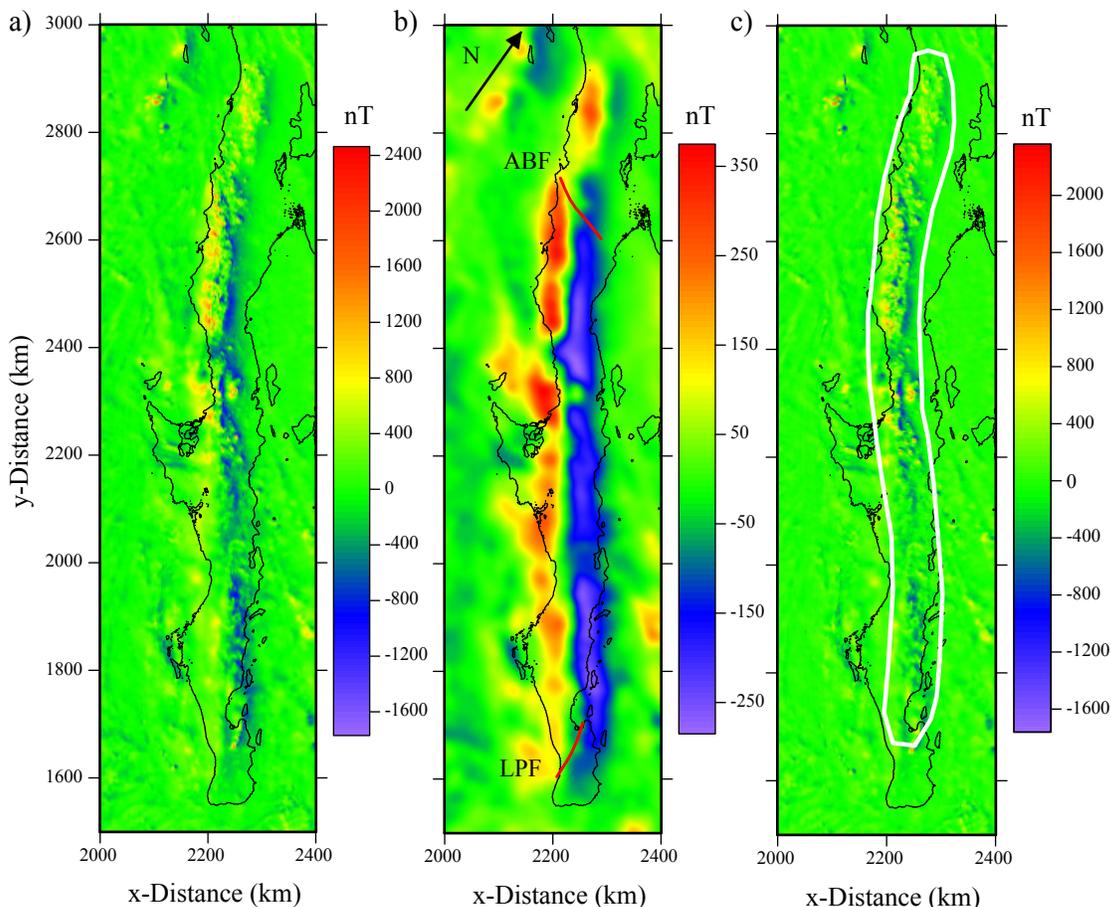

Figure 2. (a) Aeromagnetic total-field data used in this study; (b) Long-wavelength regional magnetic anomaly, where the arrow points towards geographic North, ABF denotes the Agua Blanca fault and LPF the La Paz fault; (c) Residual magnetic anomalies, the white line encloses a region characterized by high amplitude and short wavelength magnetic anomalies. Coordinates shown correspond to a Transverse Mercator projection over the central meridian -114°W, followed by a free rotation of 35 degrees clockwise.

Long-wavelength regional magnetic anomalies

As mentioned above, in previous works (Langenheim and Jachens, 2003, García-Abdeslem and Martínez-Cañedo, 2009), the amplitude and continuity of regional magnetic anomalies (Figure 2b) suggest an almost continuous belt of mafic plutons that extends over the length of the Baja California Peninsula. Also, the remarkably difference between these regional magnetic anomalies and those of low intensity observed towards the east of Peninsula, is consistent in general with a variety of hypothesis and models drawn from many geological studies, summarized and discussed by several authors (Gastil *et al.*, 1981; Sedlock *et al.*, 1993; Sedlock, 2003; Wetmore *et al.*, 2003; Busby, 2004) and from the geophysical interpretation of paleomagnetic data (Böhnel and Delgado-Argote, 2000; Schaaf *et al.*, 2000; Böhnel *et al.*, 2002; Symons *et al.*, 2003), although uncertainties, disagreements, and controversies persist, as pointed out by Sedlock (2003). It is generally agreed that during the Paleozoic and early Mesozoic, the western margin of North America was a passive continental margin where a broad platform was developed. This tectonic setting changed in Late Triassic through Early Jurassic time, when a continental magmatic arc was developed as a consequence of the subduction of the Farallon plate under the North American continent. In Early Cretaceous time, between 140 and 100 Ma (Ortega-Rivera, 2003), the active magmatic arc was located at the site of the eastern Peninsular ranges batholith. However, the differ-

ences in the chemical composition and isotopic signatures across the Peninsular batholiths are evident in mafic and magnetite-rich plutons of gabbro, norite, and tonalite on the west, and ilmenite-rich felsic plutons of granite and tonalite on the east. These differences suggest that the western Alisitos arc and the northern equivalent Santiago Peak of southern California, both, represent an island arc that evolved over an east-dipping subduction zone, accreted to the western margin of the North American continent during Late Jurassic to mid-Cretaceous time. The congenital suture of this accretion defines the magnetite-ilmenite boundary (Gastil *et al.*, 1990).

North of the Agua Blanca fault (Figure 2b), in agreement with the lateral extension of the Yuma terrain proposed by Sedlock (2003), the long wavelength magnetic anomalies are displaced eastward by about 30 km from the general trend of magnetic anomalies observed south of this fault. This slight displacement is in agreement with the right-lateral sense of motion and amount of displacement along the Agua Blanca fault in Cenozoic time (Allen *et al.*, 1960). In the region between the Agua Blanca and La Paz faults (Figure 2b), the regional magnetic anomaly has a dipolar signature, and as shown in García-Abdeslem and López-Guzmán (2009) it is likely produced by a normally magnetized, long and narrow body, and the zone of its maximum horizontal gradient is in close agreement with the Alisitos terrain as depicted by Sedlock (2003). South of the La Paz fault the dipolar signature of the regional magnetic anomaly is lost and decreases in intensity.

INVERSE MODELING LONG-WAVELENGTH MAGNETIC ANOMALIES

The inverse modeling of magnetic anomalies can yield different distributions of magnetization within the crust that may explain the observed magnetic anomalies. A preferred magnetization model (or set of models) is desired as an outcome from the inversion and this objective is made feasible by applying some regularization or physically reasonably constraints to find a particular solution to a non-unique inverse problem, as suggested in Jackson (1979) and Tarantola (2005).

The solution of the forward problem used in this work (Bhattacharyya, 1980) yields the total-field magnetic anomaly caused by a rectangular prism of constant magnetization, in the presence of the geomagnetic field. The geometry of the model used for the inversion is a cuboid that consists of a rectangular array of prismatic bodies that extends from the topography, down to 21 km below sea level. This maximum depth in the cuboid model was selected considering that it is a reasonably value for the Curie point isotherm depth, considering magnetite as the main carrier of the magnetization in the continental crust, and a 'normal' geothermal gradient of about 25 to 30 °C per km of depth. Nearby estimates of the Curie isotherm depth inferred from the spectral analysis of magnetic anomalies are available only for the region of the Sierra Cucapah and the Mexicali valley. García-Abdeslem *et al.* (2001) estimated such depth at 16 ± 2 km in the region of the Sierra Cucapah and the Mexicali valley, and recently Espinosa-Cardeña and Campos-Enríquez (2008) inferred that such depth is between 14 and 17 km at the Mexicali valley.

The prisms in the cuboid were arranged in nine layers and each layer is constituted by a regular array of 3000 prisms. Each prism has fixed horizontal dimensions, 10 km along the *x*-direction and 15 km along the *y*-direction (heading N35°E). The model parameters, *i.e.* the magnetization intensity of the prisms in the cuboid, are represented by the vector m of dimension M, which corresponds with the number of prisms in the cuboid (M = 27000).

The initial set up of the thickness of the layers in the cuboid is listed in Table 1. However the vertical extension (defined as z-Top and
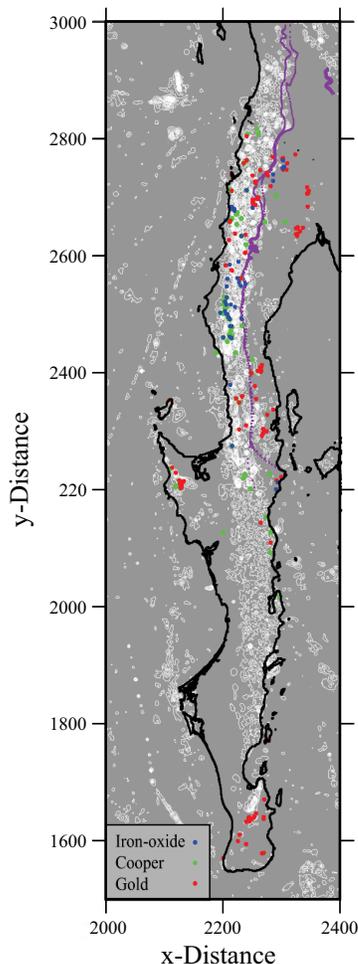

Figure 3. The 3D ASA of residual magnetic anomalies (nT/km) is shown using white isolines, the purple circles denote the magnetite-ilmenite boundary, and the location of the IOCG deposits is indicated by blue, green, and red solid circles, for iron-oxide, copper and gold deposits, respectively.

z-Bottom in Table 1) of selected prisms in layers 1 to 3 was modified to account for topographic and bathymetric features. In layers 1 and 2 the depth to the top of the prisms was defined by the height of the topography (z): layer 1 in the range of depths z <-1 km, and layer 2 in the range of depths -1< z <0 km. In layer 3, the depth to the top of the prisms is defined by the bathymetry (b): in the range of depths $0 \leq b < 3$ km.

Table 1. Initial set up of the layers that constitute the cuboid model.

Layer	z-Top (km)	z-Bottom (km)	m_p (A/m)	$1/\sigma^2$
1	-2	-1	1	100
2	-1	0	1	100
3	0	3	1	1
4	3	6	2	1
5	6	9	2	1
6	9	12	2	1
7	12	15	3	1
8	15	18	2	1
9	18	21	0	10000

The long-wavelength magnetic anomaly for the region shown in Figure 1 was selected for the inverse modeling. This data set was regularly sampled every 4 km along the x– and y– directions, and it is represented by the vector h_o of dimension N = 28500, which denotes the number of data. Correspondingly, the magnetic anomaly computed as the solution of the forward problem is denoted by the vector h of dimension N. With this notation the solution of the forward problem may be expressed as:

$$h = Am \qquad (2)$$

where each column of matrix A of dimension (N, M) represents the solution of the forward problem for a prism of unit magnetization. Assuming *a priori* gaussian probability density functions for the data and model with covariance matrices C_h and C_m, respectively, a solution to equation (1) may be found minimizing the following linear functional

$$2\phi(m)=||Am-h_o||^2_{C_d}+||m-m_p||^2_{C_m}+\alpha||Dm||^2 \qquad (3)$$

The right hand side of equation (3) consists of the sum of three norms:

(i) A misfit norm term weighted by $C_d=\varepsilon^2 I$, where $\varepsilon^2=lnT$ was assumed as the estimated uncertainty in the data. (ii) A model norm
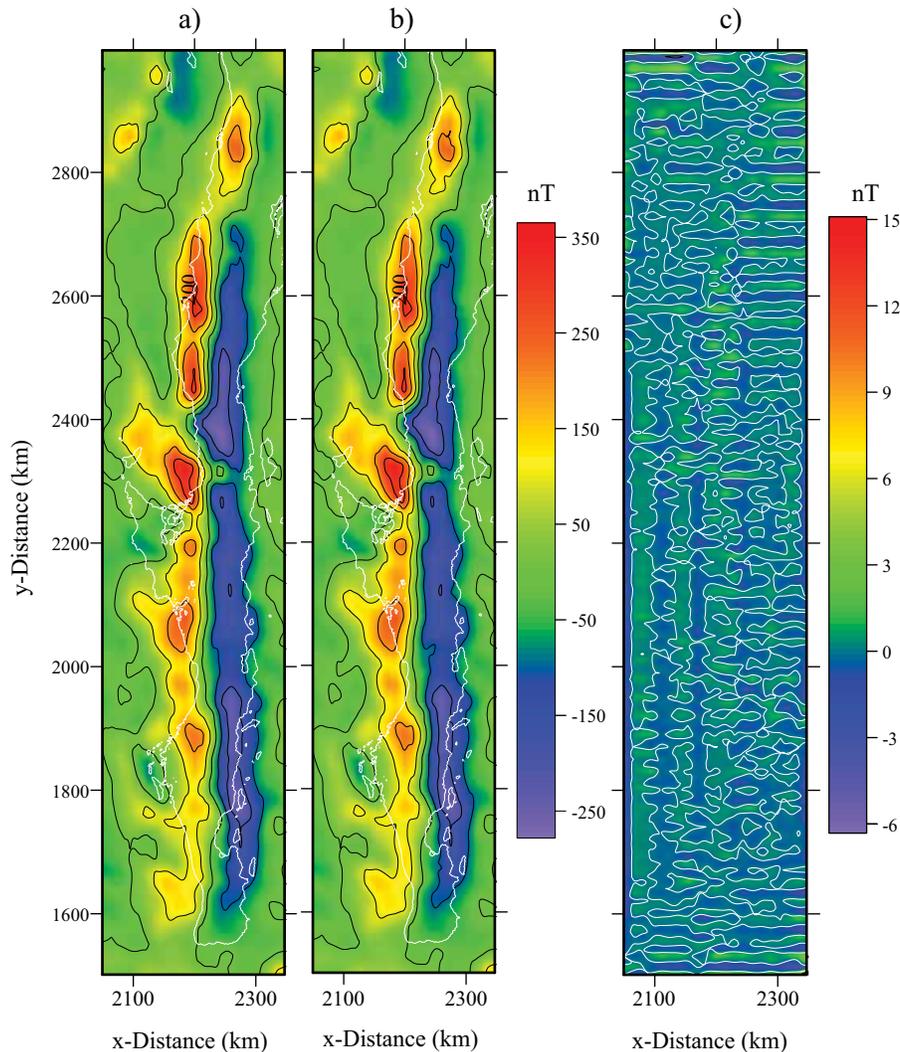

Figure 4. (a) Observed and computed (b) magnetic anomalies are shown respectively with contour lines at every 100 nT. (c) The misfit varies between -6 and 15 nT, and the zero contour is shown with a white line.

term weighted by $C_m=\sigma_j^2 I$, where FMLA σ_j assigns a level of confidence in selected elements of the prior model m_p, as well as to fixing the magnetization to some assumed value; for example, when a prism in the cuboid enclose air or seawater, the magnetization of that prism in the prior model (m_j) is defined as zero, and it is forced to remain zero by setting $\sigma_j^2=1\times10^{-9}$. (iii) A norm term that helps to impose a smooth solution, where α is a positive scalar that assigns importance to this constraint, and the matrix D of dimension (M, M) is a first derivative operator that acts upon the model along the x, y, and z directions.

Explicitly, the functional to be minimized is written as:

$$2\emptyset(m)=(Am-h_o)^T C_d^{-1}(Am-h_o)+(m-m_p)^T C_m^{-1}(m-m_p)+\alpha(Dm)^T(Dm) \quad (4)$$

Setting the $\partial\emptyset(m)/\partial m$ to zero, the solution of the inverse linear problem can be expressed as:

$$m=m_p+(A^T C_d^{-1}A+\alpha D+C_m^{-1})^{-1}A^T C_d^{-1}(h_o-Am_p) \quad (5)$$

To carry out the inverse modeling and infer the intensity of the magnetization of the prisms in the cuboid, the total-field magnetic anomaly due to the cuboid model was calculated at the continuation height, assuming induced magnetization in the direction of the geomagnetic field, with inclination (55°) and declination (10°) assumed from the IGRF epoch-2000.

Modeling results

Apart from the expected edge effect typically occurring due to the limited lateral extension of the model, that was eliminated by excluding the prims at the perimeter of the model, the results of the linear inverse modeling indicate that the long wavelength magnetic anomaly was very well explained by the inferred distribution of magnetization. Figure 4 shows the observed and computed magnetic anomalies and their misfit, which varies between -6 to 15 nT.

Figure 5 shows the lateral distribution of magnetization in layers 1 and 2. In layer 1 the magnetization is different than zero only in the highest part of the Peninsular Ranges Batholith, varying mainly in the range of ±0.004 A/m, and localized towards the east of the magnetite-ilmenite boundary. In layer 2 the negative magnetization intensity, as illustrated in Blakely (1996, p. 95), may be attributed to surface sedimentary formations in the Sebastián Vizcaíno region and along the Pacific north coast. Positive but low magnetization present elsewhere may be due to felsic volcanic rocks and volcano-sedimentary sequences with some disseminated magnetic minerals (see Table 2). Obviously, petrophysical and paleomagnetic data are needed to sustain this qualitative interpretation of the inverse modeling results.

The lateral distribution of magnetization intensity is shown in Figure 6 at selected depths between 1 and 21 km depth. 3D perspective views in Figure 7 display the magnetization intensity on several orthogonal planes, along with some selected isosurfaces of constant magnetization intensity.

Over the western portion of southern California and Baja California, two strongly magnetized belts are prominent, the northern belt is a linear feature that extends from Sebastián Vizcaino up to the Agua Blanca fault, where the northern portion of belt is easterly displaced, and coincides with the location of the Yuma Terrain (Sedlock, 2003).

In the west-central portion of the Peninsula, near the Sebastián Vizcaino region (Figure 1), the magnetization decreases drastically. In this region, geochronology and geochemical studies have shown that Cenozoic volcanic fields in the region are characterized by magnesian basaltic-andesite and adakites. This geochemical signature first suggested the possibility of ridge subduction in middle Miocene time, followed by the formation of an asthenospheric window (Aguillón-
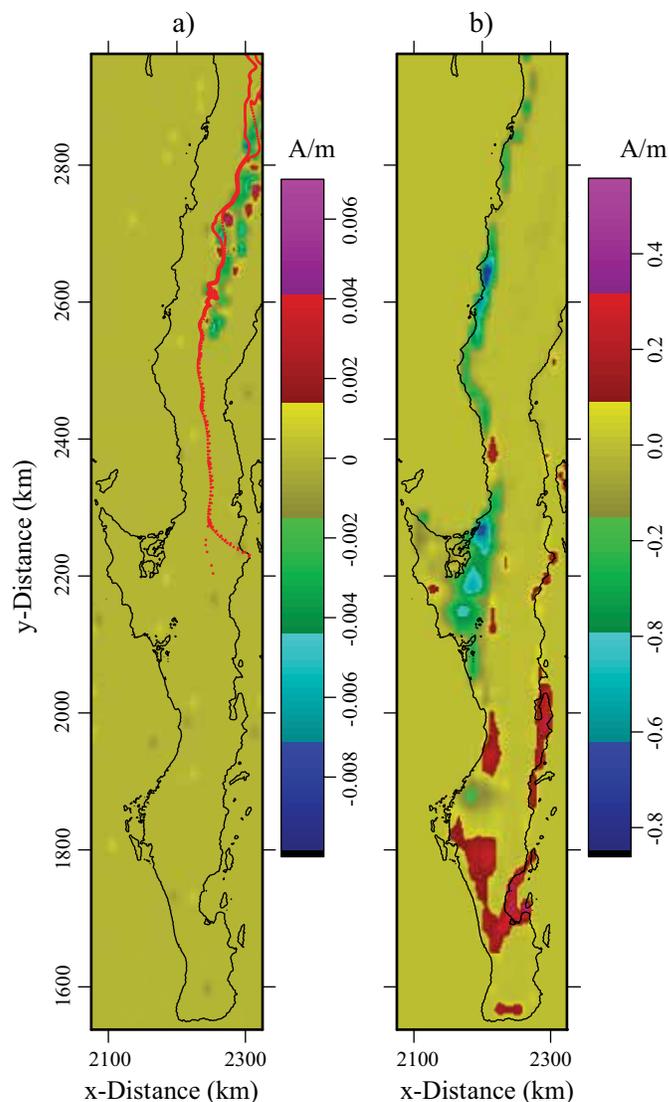

Figure 5. Plan view of the magnetization model for layer 1 (a) and layer 2 (b). The red symbols in (a) show the location of the magnetite-ilmenite boundary.

Robles *et al.*, 2001; Burgois and Michaud, 2002; Calmus *et al.*, 2003). However, such interpretation was found to be inconsistent with the occurrence of abandoned spreading centers inferred by Lonsdale (1991) off Sebastián Vizcaíno. More recently, an alternative interpretation, that takes into account geophysical characteristics of the Pacific margin off the Vizcaíno region, has suggested the possibility of an asthenospheric window on the underlying plate, due to a tearing of the subducted slab following the ridge-trench collision (Pallares *et al.*, 2007).

South of Sebastián Vizcaíno the southern belt extends linearly down to the La Paz fault, but at the southern tip of the Baja California Peninsula the magnetization model is characterized by a sharp transition from high to low magnetization across the La Paz fault. This change in magnetization intensity supports inferences, based on geochemical, isotopic, and paleomagnetic data, made by Schaaf *et al.* (2000), suggesting that the Los Cabos block has a magmatic affinity with the Puerto Vallarta batholith in mainland México, and has an independent palaeogeographical evolution with respect of rest of the Baja California Peninsula – the La Paz fault being the possible accretional boundary structure of the Los Cabos block.

Table 2. Magnetic susceptibility (per unit volume) in the cgs and SI systems of units, for different rock types, and their magnetization (*i.e.* magnetic dipole moment per unit volume) in the SI system of units, assuming an intensity of the geomagnetic field of 45000 nT.

Type	κ_v (cgs)	κ_v (SI)	M (A/m)
Sedimentary rocks	0.00005	0.0006	0.0225
Metamorphic rocks	0.0003	0.0037	0.1350
Granite and rhyolite	0.0005	0.0062	0.2250
Gabbro and basalt	0.006	0.0754	2.7002
Ultrabasic rocks	0.012	0.1508	5.4005

Another interesting feature of the model is the negative magnetization intensity found in the middle crust, east of the magnetite-imenite boundary where batholiths are rich in ilmenite. This negative feature is interpreted as due to remanent magnetization, possible caused by ilmenite-hematite solid solutions. When ilmenite is associated with hematite, *i.e.* as ilmenite-hematite lamellae, this solid solution displays self-reversed magnetization, that is, the spontaneous magnetization occurring as the rock is cooled below its Curie temperature opposes the geomagnetic field. Recent literature on this subject is abundant (Goguitchaichvili and Prévot, 2000; Prévot *et al.*, 2001; Robinson *et al.*, 2002; Kasama *et al.*, 2004; Wilson *et al.* 2005, Robinson *et al.*, 2012), but the exact mechanism of this phenomenon remains a matter of debate. However, it is generally agreed that lamellar magnetism in the hematite-ilmenite series, characterized by a hard magnetic memory, is responsible for many remanence-dominated anomalies and is a possible source for some deep crustal magnetic anomalies.

To identify the magnetization value with a rock type, the results of the inverse modeling expressed as magnetization values in A/m were converted into magnetic susceptibilities in SI units, assuming a geomagnetic field intensity of 45000 nT and compared in Figure 8 with a broad range of lithologies. This comparison suggests that regional magnetic anomalies are likely caused by a combination of gabbro and granite I-type of the magnetite series. Values of magnetic susceptibility and magnetization for some lithologies are listed in Table 2.
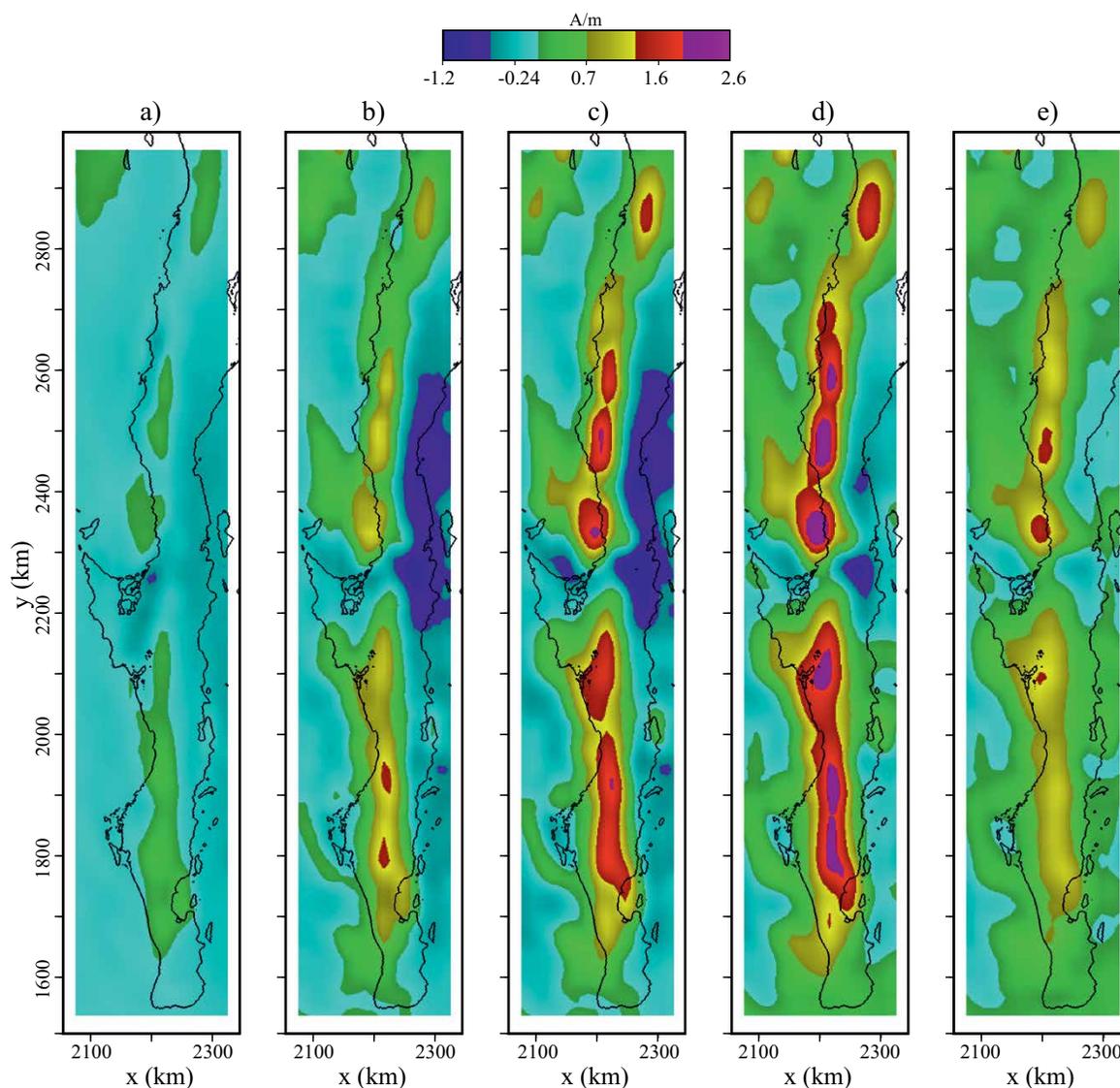

Figure 6. Plan views of the magnetization model. From (a) to (e) is shown the cuboid model at 1, 6, 11, 16, and 21 km depth, below sea level respectively.
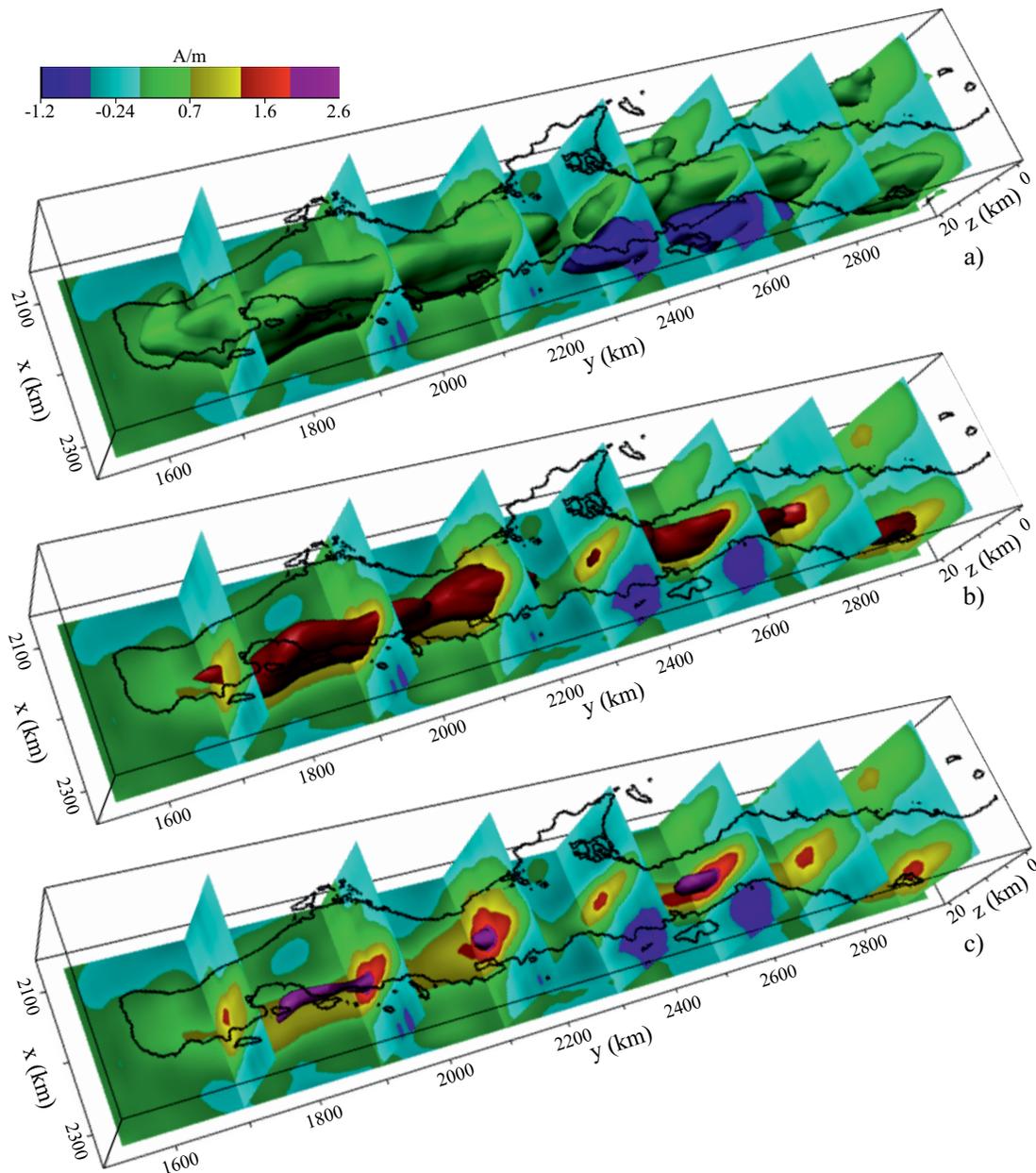
Figure 7. 3D perspective views of the magnetization intensity in the cuboid model, with a vertical exaggeration of 10, including the bottom projection at 21 km depth and seven transverse projections separated apart by 200 km. The green and blue isosurfaces shown in (a) respectively correspond to magnetization intensities of 0.69 and -0.69 A/m; in (b) the red isosurface represents a magnetization intensity of 1.3 A/m; in (c) the purple isosurface denotes a magnetization intensity of 2 A/m.

CONCLUSIONS

The 3D *ASA* of the short-wavelength residual magnetic anomalies outline shallow and strongly magnetized regions along a ~ 60 km-wide and 1200 km-long band that extends from southern California to just south of La Paz. The amplitude of both the residual magnetic anomalies and the 3D *ASA* are greater in the northern portion of this band, where most IOCG ore deposits are located.

The inverse modeling of the regional magnetic anomalies indicates that all along southern California and the western side of the Baja California Peninsula there are two fairly continuous belts of strongly magnetized rocks of mafic to intermediate composition, possible gabbro and I-type granite of the magnetite series. The boundary between these two belts is located nearby Sebastián Vizcaíno, in a region where magnetization decreases. The model shows a sharp transition from high to low magnetization across La Paz fault. Over the eastern portion of the Peninsula, a long belt is characterized by negative magnetization intensity, which is interpreted as due to remanent magnetization, possible caused by hematite-ilmenite solid solutions.
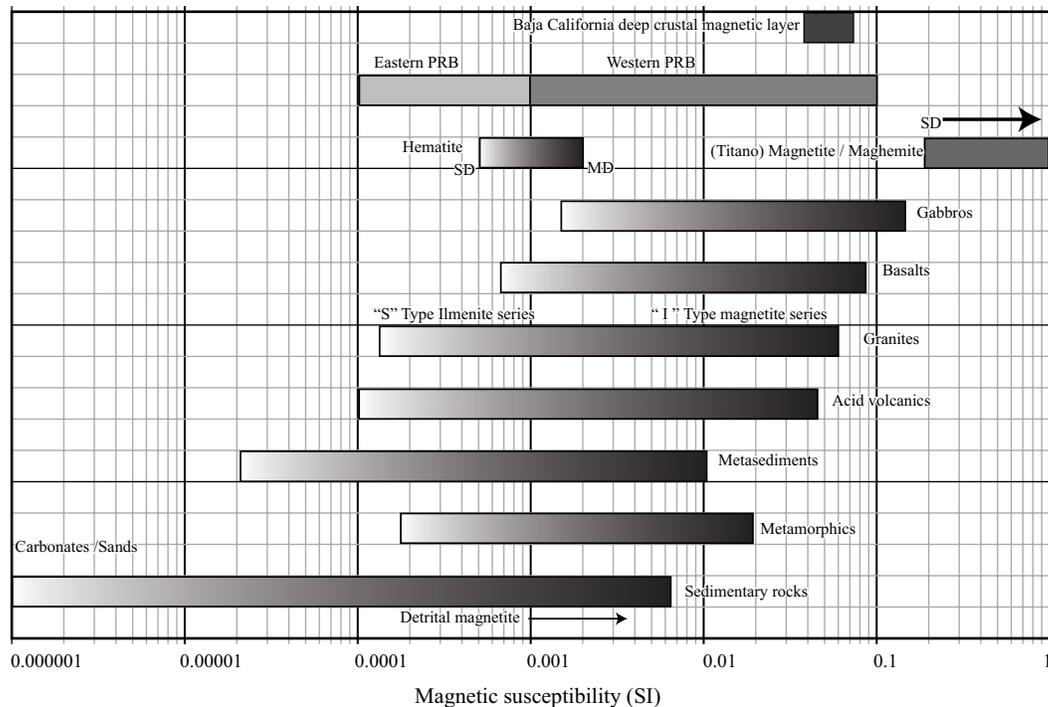
ACKNOWLEDGEMENTS

Figure 8. Magnetic susceptibility for a variety of lithologies (adapted from Clark and Emerson, 1991), showing also the susceptibilities reported by Gastil *et al.* (1991) for the PRB, and the susceptibility of the magnetized belts inferred from inverse modeling. SD = single-domain, MD = multi-domain.

REFERENCES

Aguillón-Robles, A., Calmus, T., Benoit, M., Bellon, H., Maury, R. C., Cotten, J., Bourgois, J., Michaud, F., 2001, Late Miocene adakites and Nb-enriched basalts from Vizcaíno Peninsula, México: indicators of East Pacific Rise subduction below southern Baja California?: Geology, 29, 531-534.

Allen, C.R., Silver, L.T., Stehli, F.G., 1960, Agua Blanca Fault–a major transverse structure of northern Baja California, Mexico: Geological Society of America Bulletin, 71, 467-482.

Baranov, V., 1957, A new method for interpretation of aeromagnetic maps – Pseudo-gravimetric anomalies: Geophysics, 22(2), 359-383.

Bhattacharyya, B.K., 1980, A generalized multibody model for inversion of magnetic anomalies: Geophysics, 45(2), 255-270.

Blakely, R.J., 1996, Potential Theory in Gravity and Magnetic Applications: Cambridge University Press, 441 p.

Böhnel, H., Delgado-Argote, L.A., 2000, Paleomagnetic data from northern Baja California (Mexico): results from the Cretaceous San Telmo batholith: Geological Society of America Special Paper, 334, 157-165.

Böhnel, H., Delgado-Argote, L.A., Kimbrough, D.L., 2002, Discordant paleomagnetic data for middle-Cretaceous intrusive rocks from northern Baja California: Latitude displacement, tilt or vertical axis rotation?: Tectonics, 21(5), 13-1-13-12.

Bourgois, J., Michaud, F., 2002, Comparison between the Chile and Mexico triple junction areas substantiates slab window development beneath northwesten Mexico during the past 12 Myr: Earth and Planetary Sciences Letters, 201, 35-44.

Busby, C., 2004, Continental growth at convergent margins facing large ocean basins: a case study from Mesozoic convergent-margin basins of Baja California, Mexico: Tectonophysics, 392, 241-277.

Calmus, T., Aguillón-Robles, A., Maury, R.C., Bellon, H., Benoit, M., Cotten, J., Bourgois, J., Michaud, F., 2003, Spatial and temporal evolution of basalts and magnesian andesites ("bajaites") from Baja California, Mexico: the role of slab melts: Lithos, 66, 77-105.

Clark, D.A., Emerson, D.W., 1991, Notes on rock magnetization characteristics in applied geophysical studies: Exploration Geophysics, 22, 547-555.

CRM (Consejo de Recursos Minerales), 1999a, Monografía Geológico-Minera del Estado de Baja California: Pachuca, Hidalgo, México, 182 p.

CRM (Consejo de Recursos Minerales), 1999b, Monografía Geológico-Minera del Estado de Baja California Sur: Pachuca, Hidalgo, México, 259 p.

Espinosa-Cardeña, J.M., Campos-Enríquez, J.O., 2008, Curie point depth from spectral analysis of aeromagnetic data from Cerro Prieto geothermal area, Baja California, Mexico: Journal of Volcanology and Geothermal Research, 176, 601-609.

García-Abdeslem, J., López-Guzmán, M., 2009, A suggested reverse geomagnetic polarity event inferred from the Panga de Abajo magnetic anomalies in the Mexicali Valley, Baja California, México: Geofísica Internacional, 48, 279-296.

García-Abdeslem, J., Martínez-Cañedo, P., 2009, Anomalías magnéticas, la provincia de magnetita, y su relación con yacimientos de minerales metálicos en la Península de Baja California, México: Geomimet, 278, 20-28.

Gastil, R.G., Morgan, G.J., Krummenacher, D., 1981, The tectonic history of Peninsular California and adjacent Mexico, *in* Ernst, W.G. (ed.), The geotectonic development of California (Rubey Volume I): Englewood Cliffs, N.J., Prentice-Hall, 284-306.

García-Abdeslem, J., Espinosa-Cardeña, J.M., Munguía-Orozco, L., Wong-Ortega, V.M., Ramírez-Hernández, J., 2001, Crustal structure from 2D gravity and magnetics data modeling, magnetic power spectrum inversion, and seismotectonics in the Laguna Salada basin, northern Baja California, México: Geofísica Internacional, 40, 67-85.

Gastil, G., Diamond, J., Knaak, C., Walawender, M., Marshall, M., Boyles, C., Chadwick, B., 1990, The problem of the magnetite/ilmenite boundary in

southern and Baja California, *in* The nature and origin of the Cordilleran magmatism: Geological Society of America Memoir, 174, 119-132.

Goguitchaichvili, A., Prévot, M., 2000, Magnetism of oriented single crystals of hemoilmenite with self-reversed thermoremanent magnetization: Journal of Geophysical Research, 105, 2761–2780.

Hinze, W.J., 1990, The role of gravity and magnetic methods in engineering and environmental studies, *in* Geotechnical and Environmental Geophysics, I: Society of Exploration Geophysicists, Investigations in Geophysics, 5, 75-126.

Ishihara, S., 1977, The magnetite and ilmenite-series granitic rocks: Mining Geology, 27, 293-305.

Ishihara, S., 2003, Metallogenic mineralization *vs* the granite series in the Mesozoic-Cenozoic Circum-Pacific plutonic belts *in* Blevin, P., Jones, M., Chappell, B. (eds.), Magmas to Mineralization: The Ishihara Symposium on granites and related metallogenesis, Macquarie University, Australia, 77-80.

Jackson, D.D., 1979, The use of a priori data to resolve non uniqueness in linear inversion: Geophysical Journal of the Royal Astronomical Society, 57(1), 137-157.

Kasama, T., McEnroe, S.A., Ozaki, N., Kogure, T., Putnis, A., 2004, Effects of nanoscale exsolution in hematite–ilmenite on the acquisition of stable natural remanent magnetization: Earth and Planetary Science Letters, 224, 461-475.

Langenheim, V. E., Jachens, R. G., 2003, Crustal structure of the Peninsular Ranges batholith from magnetic data: Implications for Gulf of California rifting: Geophysical Research Letters, 30(11), 1597, doi:10.1029/2003GL017159.

Lara-Sánchez, J., 2000, Avance del cubrimiento aeromagnético de la República Mexicana: GEOS, 20, 184-185.

Li, X., 2006, Understanding 3D analytic signal amplitude: Geophysics, 71(2), L13-L16.

Li, Y., Oldenburg, D.W., 1998, Separation of regional and residual magnetic field data: Geophysics, 63(2), 431-439.

Lonsdale, P., 1991, Structural patterns of the Pacific seafloor offshore of Peninsular California, *in* Dauphin, J.P., Simoneit, B. (eds.), The Gulf and Peninsular Province of the Californias: American Association of Petroleum Geologist Memoir, 47, 87-125.

NAMAG (North American Magnetic Anomaly Group), 2002, Vankey, V., Cuevas, A., Daniels, D., Finn, C.A., Hernández, I., Hill, P., Kucks, R., Miles, W., Pilkington, M., Roberts, C., Roest, W., Rystom, V., Shearer, S., Snyder, S., Sweeney, R., Vélez, J., Phillips, J., Ravat, D.G.A., Digital data grids for the magnetic anomaly map of North America: Online Linkage: ftp://ftpex.usgs.gov/, consulta: 31 de enero de 2004.

Ortega-Rivera, A., 2003, Geochronological constraints on the tectonic history of the Peninsular Ranges batholith of Alta and Baja California: Tectonic implications for western Mexico, *in* Johnson, S.E., Paterson, S.R., Fletcher, J.M., Girty, G.H., Kimbrough, D.L., Martín-Barajas, A. (eds.), Tectonic Evolution of Western Mexico and the Southwestern USA: Geological Society of America Special Paper, 374, 297-335.

Pallares, C., Maury, R.C., Bellon, H., Royer, J.-Y., Calmus, T., Aguillón-Robles, A., Cotten, J., Benoit, M., Michaud, F., Bourgois, J., 2007, Slab-tearing following ridge-trench collision: Evidence from Miocene volcanism in Baja California, Mexico: Journal of Volcanology and Geothermal Research 161, 95-117.

Prévot, M., Hoffman, K.A., Goguitchaichvili, A., Doukhan, J.C., Shcherbakov, V., Bina, M., 2001, The mechanism of self-reversal of thermoremanence in natural hemoilmenite crystals: new experimental data and model: Physics of the Earth and Planetary Interiors, 126, 75–92.

Robinson, P., Harrison, R.J., McEnroe, S.A., Hargraves, R.B., 2002, Lamellar magnetism in the haematite-ilmenite series as an explanation for strong remanent magnetization: Nature, 418, 517-520.

Robinson, P., Harrison, R.J., Fabian, K., McEnroe, S.A., 2012, Chemical and magnetic properties of rapidly cooled metastable ferri-ilmenite solid solutions: implications for magnetic self-reversal and exchange bias—III. Magnetic interactions in samples produced by Fe–Ti ordering: Geophysical Journal International, 191, 1025-1047.

Schaaf, P., Böhnel, H., Pérez-Venzor, J.A., 2000, Pre-Miocene paleogeography of the Los Cabos Block, Baja California Sur: geochronological and paleomagnetic constrains: Tectonophysics, 318, 53-69.

Sedlock, R.L., 2003, Geology and tectonics of the Baja California Peninsula and adjacent areas, *in* Johnson, S.E., Paterson, S.R., Fletcher, J.M., Girty, G.H., Kimbrough, D.L., Martín-Barajas, A. (eds.), Tectonic Evolution of Western Mexico and the Southwestern USA: Boulder, Colorado, Geological Society of America Special Paper, 374, 1-42.

Sedlock, R.L., Ortega-Gutiérrez, F., Speed, R.C., 1993, Tectonostratigraphic terranes and tectonic evolution of Mexico: Geological Society of America Special Paper, 278, 153 p.

Symons, D.T.A., Walawander, M.J., Smith, T.E., Molnar, S.E., Harris, M.J., Blackburn, W.H., 2003, Paleomagnetism and geobarometry of La Posta Pluton, California, *in* Johnson, S.E., Paterson, S.R., Fletcher, J.M., Girty, G.H., Kimbrough, D.L., Martín-Barajas, A. (eds.), Tectonic Evolution of Western Mexico and the Southwestern USA: Boulder, Colorado, Geological Society of America Special Paper, 374, 135-155.

Tarantola, A., 2005, Inverse Theory and Methods for Model Parameter Estimation: Society for Industrial and Applied Mathematics, 342 p.

Tarling, D.H., 1983, Paleomagnetism: principles and applications in Geology, Geophysics and Archaeology: London, New York, Chapman and Hall, 379 p.

USGS (United States Geological Survey), 2010, Geologic Map of North America: <http://ngmdb.usgs.gov/gmna/>, consulta: 26 de junio de 2011.

Wetmore, P.H., Herzig, C., Alsleben, H., Sutherland, M., Schmidt, K.L., Schultz, P.W., Paterson, S.R., 2003, Mesozoic tectonic evolution of the Peninsular Ranges of southern and Baja California, *in* Johnson, S.E., Paterson, S.R., Fletcher, J.M., Girty, G.H., Kimbrough, D.L., Martín-Barajas, A. (eds.), Tectonic Evolution of Western Mexico and the Southwestern USA: Boulder, Colorado, Geological Society of America Special Paper, 374, 93-116.

Wilson, N.C., Muscat, J., Mkhonto, D., Ngoepe, P.E., Harrison, M., 2005, Structure and properties of Ilmenite from first principles: Physical Review, B 71, 075202, DOI:10.1103/PhysRevB.71.07520.